Biochimica et Biophysica Acta 1848 (2015) 444–452

Contents lists available at ScienceDirect

Biochimica et Biophysica Acta

journal homepage: www.elsevier.com/locate/bbamem

Membrane activity of the pentaene macrolide didehydroroflamycoin in model lipid bilayers

Alena Koukalová [a,b], Šárka Pokorná [a], Radovan Fišer [b,c], Vladimír Kopecký Jr. [d], Jana Humpolíčková [a,*], Jan Černý [b], Martin Hof [a]

[a] J. Heyrovský Institute of Physical Chemistry, Academy of Sciences of the Czech Republic, v.v.i., Dolejškova 2155/3, 182 23 Prague 8, Czech Republic
[b] Faculty of Science, Charles University in Prague, Albertov 6, 128 43 Prague 2, Czech Republic
[c] Institute of Microbiology, Academy of Sciences of the Czech Republic, v.v.i., Vídeňská 1083, 142 20 Praha 4-Krč, Czech Republic
[d] Institute of Physics, Faculty of Mathematics and Physics, Charles University in Prague, Ke Karlovu 5, 121 16 Prague 2, Czech Republic

ARTICLE INFO

Article history:
Received 26 June 2014
Received in revised form 21 October 2014
Accepted 27 October 2014
Available online 4 November 2014

Keywords:
Didehydroroflamycoin
Filipin III
Amphotericin B
Giant unilamellar vesicles
Cholesterol

ABSTRACT

Didehydroroflamycoin (DDHR), a recently isolated member of the polyene macrolide family, was shown to have antibacterial and antifungal activity. However, its mechanism of action has not been investigated. Antibiotics from this family are amphiphilic; thus, they have membrane activity, their biological action is localized in the membrane, and the membrane composition and physical properties facilitate the recognition of a particular compound by the target organism. In this work, we use model lipid membranes comprised of giant unilamellar vesicles (GUVs) for a systematic study of the action of DDHR. In parallel, experiments are conducted using filipin III and amphotericin B, other members of the family, and the behavior observed for DDHR is described in the context of that of these two heavily studied compounds. The study shows that DDHR disrupts membranes via two different mechanisms and that the involvement of these mechanisms depends on the presence of cholesterol. The leakage assays performed in GUVs and the conductance measurements using black lipid membranes (BLM) reveal that the pores that develop in the absence of cholesterol are transient and their size is dependent on the DDHR concentration. In contrast, cholesterol promotes the formation of more defined structures that are temporally stable.

1. Introduction

Polyene macrolides are biologically active metabolites isolated from *Streptomyces* [1]. Due to their antifungal activity, some of them, e.g., amphotericin B (AmB) or nystatin, have been used in human medicine to treat fungal infections for several decades [2]. Their mode of action is assumed to heavily involve biological membranes [3]. Although polyene antibiotics share a similar structure, the mechanism of the interaction with the membrane can substantially differ and cannot be easily predicted. For instance, AmB and nystatin form ion channel pores [3], but the pentaene filipin III acts as a general disruptor through membrane protrusions that arise from altered phase behavior [4–6]. The action of most polyenes strongly depends on the presence of sterols in membranes [7–10]. Furthermore, a target organism can be identified by the sterol composition of its membrane [11], and despite the importance of sterols, the involvement of sterols is not thoroughly understood. Pore formation occurs even in sterol-free bilayers, indicating that sterols merely facilitate the incorporation of antibiotics into the membrane via modulation of the membrane mechanical properties [6,12]. In contrast, specific interactions of the mycosamine moiety of AmB have been proposed to be crucial for the interaction with ergosterol [13].

In this manuscript, we investigate the membrane interactions of a recently isolated polyene macrolide, 32,33-didehydroroflamycoin (DDHR, Fig. 1) [14]. To date, the only known aspect of its mechanism of action is associated with the dose-dependent hemolysis of red blood cells [15].

In this study, leakage assays were used to study the creation of pores, as well as other membrane formations (buds, non-spherical shape), in well-defined, free-standing model membranes of giant unilamellar vesicles (GUVs). In particular, we focus on the role of cholesterol and its participation in the enhancement/attenuation of membrane disruption. By combining these assays with conductance measurements of black lipids membranes (BLMs), we demonstrate that the pores formed in cholesterol-containing bilayers are defined in size and temporally stable. In contrast, the pores formed in the absence of cholesterol resemble general membrane disruptions, which are transient and whose size depends on the concentration.

Furthermore, we study membranes consisting of coexisting fluid phases and the ability of DDHR to promote these phases in a homogeneous bilayer. Additionally, experiments are also performed using filipin III and AmB (Fig. 1), other members of the polyene macrolide

* Corresponding author. Tel.: +420 266 053 142; fax: +420 286 58 2 307.
E-mail address: jana.humpolickova@jh-inst.cas.cz (J. Humpolíčková).

http://dx.doi.org/10.1016/j.bbamem.2014.10.038
0005-2736/

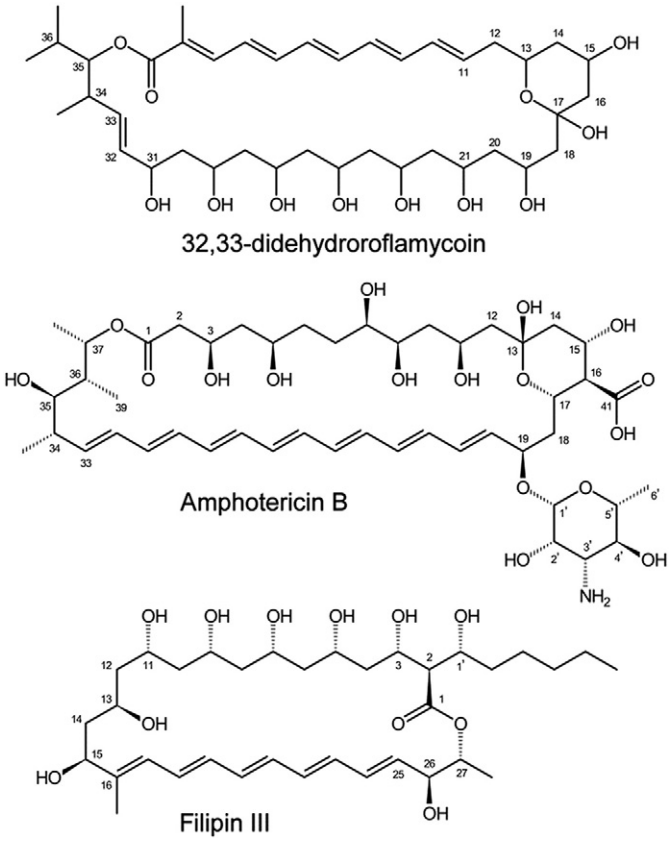

Fig. 1. Structures of the polyene macrolides 32,33-didehydroroflamycoin, amphotericin B and filipin III.

family. The similarities and differences in their action are demonstrated, showing that although cholesterol substantially participates in the action of all the presented antibiotics, its final effect on the fate of a membrane and potentially on the fate of a cell may be very different.

2. Materials and methods

2.1. Extraction of DDHR and other macrolides

Dry DDHR powder was kindly gifted by the Laboratory of Fungal Genetics and Metabolism (Institute of Microbiology, Academy of Sciences of the Czech Republic v.v.i., Prague, Czech Republic). The extraction procedure has been described elsewhere [14]. The dry DDHR powder was kept in the dark at −20 °C. A stock solution of 5 mM DDHR was prepared by dissolving the DDHR powder in methanol. This solution was stored as aliquots at −80 °C and was protected from light. Pure methanol was used as a solvent due to the poor solubility of DDHR in water. Additionally, 5 mM stock solutions of AmB and filipin III were prepared in methanol.

2.2. Solvent and reagents

1,2-Dioleoyl-sn-glycero-3-phosphocholine (DOPC), porcine brain sphingomyelin (Sph) and cholesterol were purchased from Avanti Polar Lipids Inc. (Alabaster, AL). All lipids were used without purification after the phospholipid purity was confirmed using thin-layer chromatography. Stock solutions were prepared in chloroform using standard quantitative techniques. Atto488 was purchased from ATTO-Tec (Siegen, Germany) and prepared as a stock solution in 105 mOsm glucose buffer. DiIC18(5) (DiD), AlexaFluor®488-labeled dextran 3000 and dextran 10 000 were purchased from Life Technologies Corporation (Carlsbad, CA), and the dextrans were dissolved in 105 mOsm glucose buffer. Filipin III and AmB were purchased from Sigma-Aldrich (St. Louis, MO).

2.3. GUV formation

GUVs were prepared using a modified electroformation method originally developed by Angelova [16]. Lipid mixtures were prepared from stock solutions in chloroform. The total amount of all lipids (100 nmol in approximately 200 μL of chloroform) together with DiD (0.1 mol%) was spread onto two hollowed titanium plates, which were placed on a heater plate at approximately 50 °C to facilitate solvent evaporation, and the mixture was subsequently placed in high vacuum for at least 1 h for evaporation of the remaining solvent traces. The lipid-coated plates were assembled using one layer of Parafilm for insulation [17]. The electroswelling chamber was filled with 1 mL of preheated sucrose solution (100 mM sucrose, osmolarity of 103 mOsm/kg) and sealed with Parafilm. An alternating electrical field of 10 Hz that increased from 0.02 V to 1.1 V (peak-to-peak voltage) during the first 45 min was applied and was then maintained at 1.1 V for an additional 2.5 h at 55 °C; this field was followed by 30 min of 4 Hz and 1.3 V to detach the formed liposomes. Finally, approximately 40 μL of the GUV suspension was placed in a microscopy chamber containing 360 μL of glucose buffer (~80 mM glucose, 10 mM HEPES and 10 mM NaCl, pH 7.2) with an osmolarity of 103 mOsm/kg. The presence of glucose in the final solution allowed the liposomes to sediment and decreased the vesicle movement.

For all the experiments, DDHR, filipin III and AmB were added to the glucose buffer prior the addition of GUVs. For the leakage assays, the glucose buffer also contained Atto488, labeled dextrans or methanol in the desired concentration. The leaking vesicles were counted after 1 h of incubation. All the measurements were performed at room temperature.

Simultaneously with the leakage experiments, control experiments were conducted. Instead of DDHR or the other investigated polyenes, methanol in the same volume as the volume of the polyene solution was added. The maximum methanol volume fraction was 1%. The control GUVs were stable, as shown in Table 1.

2.4. LUV formation

For LUV formation, an appropriate mixture containing 10^{-6} mol of lipids was prepared in chloroform. Chloroform was evaporated using a rotary evaporator, and the lipid film was rehydrated using 1 mL of buffer solution (10 mM HEPES, 150 mM NaCl and 2 mM EDTA, pH 7). A turbid solution containing the multilamellar vesicles was extruded 10 times using 100 nm filters in a LIPEX extruder (Northern Lipids Inc., Canada) [18].

2.5. Absorption/emission spectra

Absorption spectra were measured on a UV2600 UV–VIS spectrophotometer (Shimadzu Corporation, Kyoto, Japan). Emission spectra were monitored using a FluoroLog 3 steady-state fluorescence spectrometer (model FL3-11; Horiba Jobin Yvon Inc., Edison, NJ). DDHR was excited by 370 nm light.

2.6. Confocal microscopy

Confocal microscopy imaging was performed on an FV1000 (Olympus, Hamburg, Germany), and the microscope was equipped with a UPLSAPO 60× W N.A. 1.20 objective lens. Atto488, AlexaFluor®488 and DiD were excited using the 488 and 632 nm laser lines, respectively. DDHR and filipin III was excited by a Coherent Chameleon Vision II titanium:sapphire laser (Coherent, Santa Clara, CA) using multiphoton excitation at 800 and 750 nm, respectively.

Table 1
Percentage of leaking GUVs exposed to three different concentrations of DDHR (mean ± standard deviation) and the control experiments. The numbers in parenthesis indicate the number of analyzed GUVs/number of independent measurements. The mean values and standard deviations are calculated from subsets of the analyzed GUVs (100 GUVs each).

	10 μM DDHR		30 μM DDHR				50 μM DDHR		Controls			
	DOPC	DOPC/Chol (7/3)	DOPC	POPC	DOPC/Chol (7/3)	DOPC/Sph/Chol (2/2/1)	DOPC	DOPC/Chol (7/3)	DOPC	POPC	DOPC/Chol (7/3)	DOPC/Sph/Chol (2/2/1)
Atto488	12 ± 8 (>600/2)	6 ± 4 (>600/2)	84 ± 13 (>1100/4)	99 ± 1 (>600/1)	42 ± 23 (>1700/5)	56 ± 16 (>300/1)	–	–	11 ± 6 (>2800/9)	8 ± 3 (>600/1)	9 ± 7 (>2600/8)	2 ± 1 (>300/1)
Dextran 3000	–	–	9 ± 4 (>600/2)	–	6 ± 5 (>600/2)	–	78 ± 10 (>300/1)	12 ± 1 (>300/1)	6 ± 4 (>600/2)	–	3 ± 4 (>600/2)	–
Dextran 10 000	–	–	9 ± 5 (>600/2)	–	6 ± 5 (>600/2)	–	87 ± 9 (>300/1)	12 ± 9 (>300/1)	4 ± 2 (>300/1)	–	9 ± 4 (>300/1)	–

2.7. Analysis of confocal images

The obtained images were analyzed both qualitatively and quantitatively. Qualitatively, the characteristic vesicle behavior in the presence of DDHR was assigned to various patterns. This determination was based on a continuous observation of the fluorescence of the components for the first 30 min after the vesicle transfer. The images of the vesicle remained focused at the equatorial plane.

The confocal images and movies were quantitatively analyzed using ImageJ. Vesicles that appeared multilamellar or aggregated and those that had a diameter of less than 10 μm were not analyzed. When the fluorescence intensity of either Atto488 or labeled dextrans inside of the GUVs was greater than 20% of the intensity outside of the GUVs, the GUV was considered a leaking GUV. This choice corresponds to the control experiments, where up to a leaking efficiency of up to 20% was found for majority of GUVs.

2.8. FTIR spectroscopy

Infrared spectra were recorded on a Vector 33 FTIR spectrometer (Bruker Optik GmbH, Ettlingen, Germany) using a standard MIR source, KBr beamsplitter and MCT detector. The spectrometer was purged using dry air. Four thousand scans were collected at a spectral resolution 2 cm^{-1} with a Blackman-Harris 3-term apodization function. The samples were measured at room temperature (20 °C) in a CaF_2 cell with an 8-μm path length. The spectral contribution of the buffer was corrected using a standard algorithm [19], and the FTIR spectrum of water vapor was subtracted. The FTIR difference spectrum was calculated in the following manner—the spectrum of DDHR with cholesterol in complex was taken as a reference, and the spectra of the DDHR and cholesterol solution were fit to it together with a polynomial correction (7^{th} grade) of the background. The data processing was performed using GRAMS/AI 9.1 software (Thermo Scientific, Waltham, MA, USA).

Samples were prepared for FTIR by dissolving dry DDHR powder and cholesterol in deionized water containing SDS. The final concentrations in the sample were 40 mM DDHR and cholesterol 80 mM SDS. The mixtures were vortexed well to create proper micelles.

2.9. Electrophysiology

Measurements on planar lipid bilayers (black lipid membranes) were performed in Teflon cells separated by a diaphragm with a circular hole (diameter: 0.5 mm) bearing the membrane. DDHR was added to the grounded *cis* compartment that had a positive potential. The membrane was formed using the painting method with a 3% lipid solution in *n*-decane:butanol (9:1 *v*/*v*) using soybean phosphatidyl choline alone (type IIS, asolectin; Sigma-Aldrich, St. Louis, MO) or in a mixture with 30% (*w*/*w*) cholesterol (Sigma-Aldrich, St. Louis, MO). Both compartments contained 2 mL of 10 mM Tris and 1 M KCl at pH 7.4. The membrane current was recorded using Ag/AgCl electrodes (Theta) with salt bridges (applied voltage: 70 mV), amplified using LCA-4k-1G or LCA-200-100G amplifiers (Femto, Berlin, Germany) and digitized using a KPCI-3108 card (Keithly, Cleveland, OH) and BLM2 software (Assoc. Prof. Jiří Bok, Charles University in Prague, Czech Republic). The signal was processed using a Perl script and QuB software (http://www.qub.buffalo.edu/). The single-channel recordings were electronically filtered using a 30 Hz low-pass filter.

3. Results and discussion

3.1. Spectroscopic properties

The polyene motif in DDHR, as well in most other members of the family, is responsible for the fluorescence of these molecules. The absorption and emission spectra of DDHR in DOPC LUVs are shown in Fig. 2. No significant difference in the absorption/emission spectra were observed between the cholesterol-containing and cholesterol-free LUVs. This result suggests that no cholesterol-induced aggregation of DDHR occurs in the investigated concentration range (up to 50 μM), in contrast to the results for filipin III [20] and Nystatin [21]. The fluorescence signal of DDHR in buffer solution is several orders of magnitudes weaker than its signal in LUVs. This difference probably stems from a high tendency of the amphiphilic molecules to self-aggregate in polar solvents.

When visualizing GUVs containing DDHR, we utilized its fluorescence properties and two-photon excitation for imaging.

3.2. Pore-formation activity of DDHR

The main action of macrolide antibiotics is assumed to occur at the membrane surface and is attributed to the formation of membrane disruptions, specifically pores. Their structural properties may be very different, ranging from the well-defined barrel-shaped structures formed by AmB [22] to the general disruptions formed by filipin III

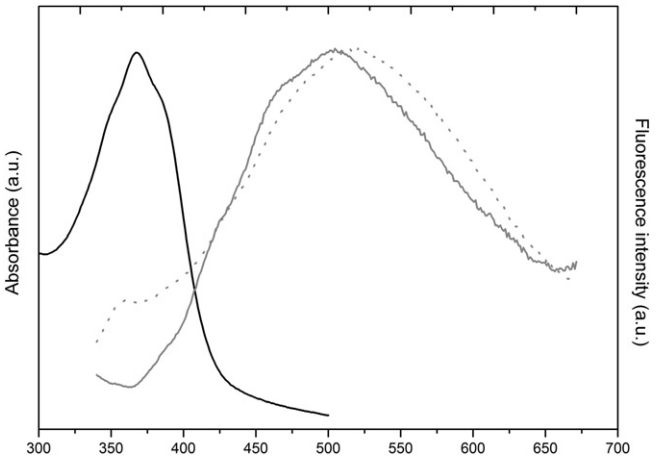

Fig. 2. Absorption (black line) and emission (grey line) spectra of DDHR in DOPC LUVs for concentrations ranging from 10 to 50 μM. The total lipid concentration was 1 mM. The dotted line shows the normalized fluorescence spectra of DDHR in HEPES buffer (very low fluorescence signal).

that have an undefined nature [6]. Because we cannot provide detailed insight into their shapes and sizes, we will concentrate on their actions, as revealed by vesicle leaking. The formation of these pores is generally dependent on the presence of sterols. Our attention therefore mainly focuses on the role of cholesterol in the pore formation at various concentrations of DDHR.

To determine the ability of DDHR to disrupt lipid membranes, we performed a leakage assay that followed the penetration of the fluorescent dye Atto488 and various sizes of labeled dextrans into GUVs composed either of pure DOPC, POPC or DOPC/cholesterol (7:3, mol/mol) upon the addition of DDHR. After the GUVs were treated with DDHR, the percentage of leaking vesicles was counted using confocal microscopy (see Table 1). The percentage of leaking GUVs reflects how prone the membrane is to disruption by the amphiphile.

The results shown in Table 1 allow for the following conclusions: first, at all tested concentrations of DDHR (30–50 μM), the GUVs that consist of pure DOPC or POPC displayed much more leaking than that of the cholesterol-containing GUVs. The leakage assays were also performed for AmB and filipin III (Table 2). The action of filipin III occurred at a much lower concentration than did the actions of DDHR and AmB. At a decreased level of filipin III (10 μM), there was almost no action in the cholesterol-free membranes, whereas the cholesterol-containing GUVs were torn into pieces and not observable any more. The action of AmB confirmed the effect of cholesterol on membrane disruption, as indicated by the elevated number of leaking GUVs in the presence of cholesterol. This finding suggests that for DDHR, cholesterol reduces leaking, in contrast to the results for the other polyene macrolides (AmB, filipin III).

Fig. 3**A** shows the distribution of the leaking efficiency (amount of intrinsic fluorescence with respect to the outside fluorescence) in the analyzed ensemble of GUVs. Both AmB and DDHR can cause leaking in cholesterol-free GUVs (nearly 100%). However, in the cholesterol-containing membranes, the leaking efficiency decreases; for AmB, the effect is only small, if any, and for DDHR, the leaking efficiency drops to 25%. This finding is most likely related to the size of the pores, which prevents the penetration of some fluorescent probes that do not have a suitable orientation when they encounter the membrane pore.

To determine whether the altered leaking properties in the system containing cholesterol can be attributed exclusively to the presence of cholesterol or whether the change arises from the increased membrane rigidity that results from the presence of sterol, we also performed an experiment using POPC GUVs. Table 1 shows that the POPC membrane, which is more ordered than the DOPC membrane [23], displays the same leaking properties as the DOPC membrane. These findings suggest that cholesterol does indeed have a specific role in pore formation.

Table 2
Percentage of leaking GUVs (mean ± standard deviation) for a comparison of the actions of filipin III and AmB with those of DDHR in cholesterol-containing and cholesterol-free GUVs. The numbers in parenthesis stand for the number of analyzed GUVs/number of independent measurements. The mean values and standard deviations are calculated from subsets of analyzed GUVs (100 GUVs each).

	DOPC	DOPC/Chol (7/3)
10 μM filipin	16 ± 5 (>300/1)	Not-measurable
30 μM AmB	44 ± 6 (>300/1)	73 ± 6 (>300/1)
50 μM AmB	76 ± 5 (>300/1)	85 ± 3 (>300/1)
10 μM DDHR	12 ± 8 (>600/2)	6 ± 4 (>600/2)
30 μM DDHR	84 ± 13 (>1100/4)	42 ± 23 (>1700/5)
Controls	11 ± 6 (>2800/9)	9 ± 7 (>2600/8)

Second, the leakage assay was performed at various concentrations of DDHR (10, 30, 50 μM). At the lowest concentration (10 μM), no significant changes in the vesicle leakage were detected compared with that in the control experiments; however, in the solution containing 30 μM DDHR, a large amount of leaking GUVs were found (~90% for pure DOPC membranes). This suggests that a certain threshold concentration must be exceeded for pore formation. Below that concentration (10 μM), DDHR incorporates into the membrane, as indicated by 2-photon microscopy, but the pores are either not created or are smaller than the size of Atto488, the dye that was used.

Third, to determine the size of the pores, we used labeled molecules with different sizes – Atto488-COOH (800 Da), dextran 3 000 (3 kDa) and dextran 10 000 (10 kDa). The results of these experiments are shown in Table 1. Different behaviors are clearly observed for the GUVs containing cholesterol and the cholesterol-free membranes. In pure DOPC, larger dextrans can penetrate the membrane when the DDHR concentration increases; however, in the GUVs containing cholesterol, neither of the two dextrans can pass through the bilayer even at increased levels of DDHR. This finding suggests that the pores formed in the presence of cholesterol have well-defined structures, whereas the pores formed in the cholesterol-free membranes are more general membrane ruptures. Fig. 3C and D shows the distributions of the leaking efficiency for differently large molecules in the cholesterol-free and cholesterol-containing membranes, respectively. The size dependence is nicely illustrated in the 30 μM DDHR system that does not contain cholesterol (Fig. 3C): Atto488 performs almost 100% leaking efficiency, but the 3 kDa dextran molecules are significantly less effective, and the 10 kDa molecules do not penetrate the membrane at all.

3.3. Pore formation observed using conductance measurements

The channel formation caused by DDHR was also examined by measuring the membrane current/conductance in BLMs. In accordance with the leakage assays, the pore formation also strongly depended on the presence of cholesterol. Notably, the stability of the BLMs without cholesterol in the presence of DDHR was already significantly lowered than that of the cholesterol-containing BLMs. The BLMs without cholesterol usually collapsed a few minutes after their creation, whereas with cholesterol the membrane was stable, at least in the time range of tens of minutes, and its conductance far exceeded the level reached in the cholesterol-free membranes. The fast collapses of the cholesterol-free BLMs occur on the same timescale as the budding-fission cycles in GUVs described in the following section; thus, we may attribute these two observations to the same phenomena. Fig. 4 depicts the time evolution of the electric current across the membrane in a pure asolectin bilayer and in an asolectin/cholesterol system. In the former case, individual pores (ion channels) are clearly distinguishable, causing defined current fluctuations when opening and closing (Fig. 5). These channels most likely contribute to the overall leaking observed in GUVs for the cholesterol-free bilayers. In the latter case, the increase in the current is continuous, and the single opening-closing events are not observable even at the initial times. This finding allows us to conclude that pores are formed transiently in the absence of cholesterol, but cholesterol-containing pores are either much smaller or temporally stable or a combination of both. The average pore conductance in the system with no cholesterol is 25 pS, which corresponds to the conductance for pores that are approximately 1 nm in diameter. The leakage assays suggest that the pores in both systems are permeable to the organic fluorophore Atto488 (in the cholesterol-containing membranes, the leaking efficiency is significantly reduced, but leaking still occurs, Fig. 3). Therefore, the cholesterol-containing pores cannot be significantly smaller than 1 nm in diameter; opening and closing events are not observed, which most likely causes the prolonged temporal stability of the pores. This explanation is consistent with the conclusion drawn from the leakage assays that

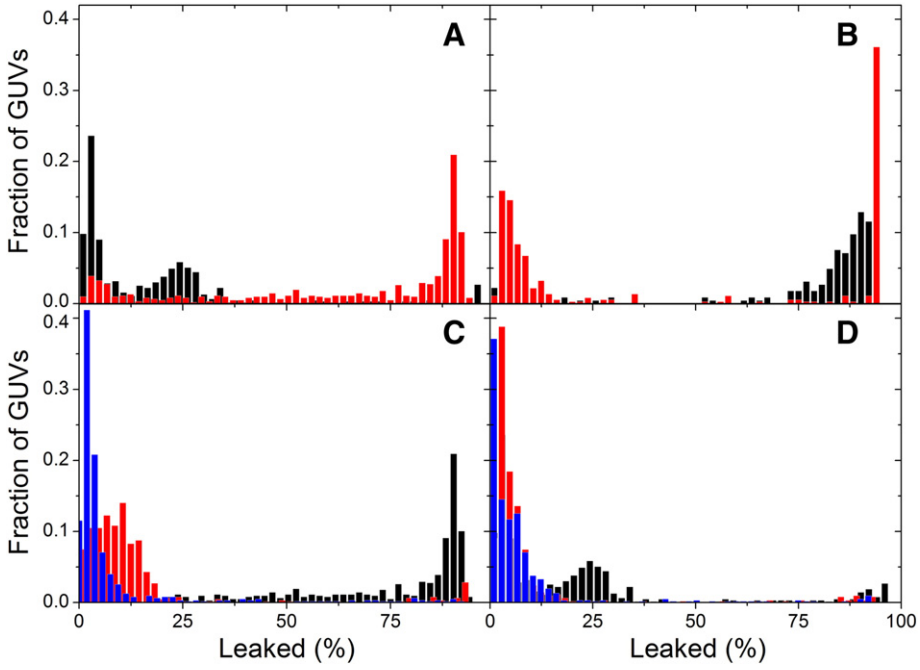

Fig. 3. Distributions of the leaking efficiency among the analyzed GUVs. A,B) Leaking of Atto488 through cholesterol-free membranes (red) and cholesterol-containing membranes (black) caused by A) 30 μM DDHR, and B) 30 μM AmB. C, D) Leaking of molecules of increasing size (Atto488: black, dextran 3 000: red, and dextran 10 000: blue) through DOPC and DOPC/chol membranes, respectively.

suggested the creation of defined complexes between DDHR and cholesterol-containing pores.

In BLMs, cholesterol seems to promote transmembrane ion transport through pores/channels; however, the leakage assays suggest lower leaking efficiency in the cholesterol-containing GUVs. The BLMs lacking cholesterol were much less stable and often ruptured early after the BLM formation. Thus, the conductance was much higher in the cholesterol-containing BLMs than in the cholesterol-free bilayer. As discussed in the following section, an additional leaking mechanism associated with morphological changes of GUVs and follow-up budding/vesicle fission cycles is most likely responsible for the overall greater disruption of the cholesterol-free membranes.

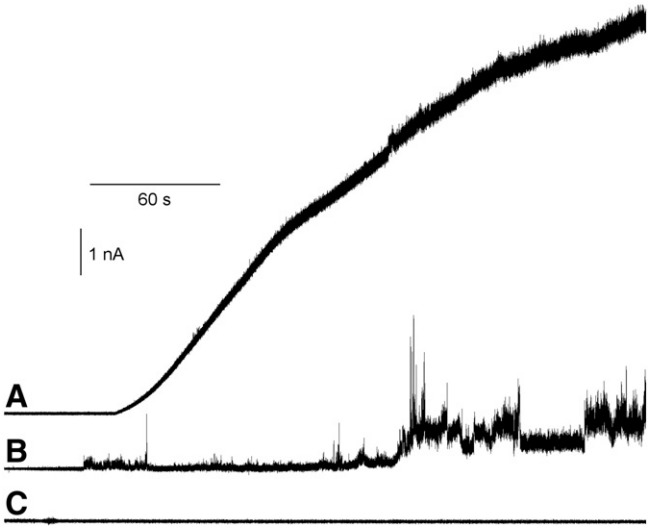

Fig. 4. Typical electrical current recordings showing the membrane conductance induced by 21 μM DDHR in (A) asolectin/cholesterol (7:3, *w*/*w*) or in (B) asolectin membranes. (C) A control trace without DDHR. The current was recorded at 70 mV in 1 M KCl and 10 mM Tris, pH 7.4.

3.4. DDHR-driven morphological changes of GUVs

At the lowest DDHR concentration, the vesicles did not undergo any deformations; however, in the higher concentration range (30 or 50 μM), the GUVs only remained spherical for a few minutes after their transfer into the measuring chambers. Later, various membrane formations evolved in the cholesterol-free GUVs. Numerous vesicles were not spherical anymore; instead, they became irregularly elongated, asymmetric and not stable in shape (Fig. 6B). However, the most commonly observed formations were groups of small disorganized spheres (Fig. 6A). The process of their formation was directly observable during the experiment. In the beginning, the small spheres were formed as individual buds, followed by their fission from the membrane of the mother GUV. This cycle repeated several times, and as additional smaller spheres evolved, the GUVs leaked more rapidly. This behavior was not observed for either AmB of filipin III.

Morphological changes and sphere formation are often attributed to an asymmetric localization of the amphiphile [24]. When the amphiphile inserts into the outer leaflet, it causes membrane stress. This stress calls for an effective translocation mechanism that allows access to the

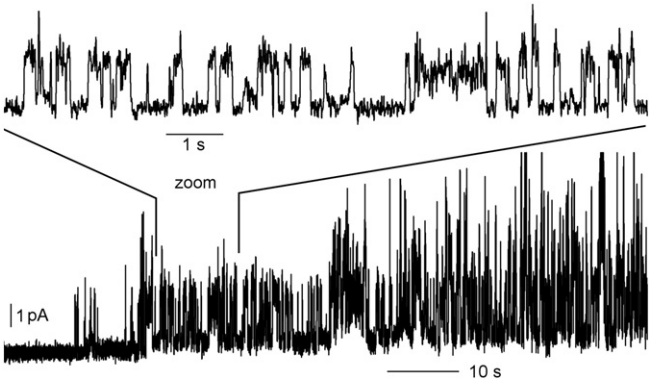

Fig. 5. Representative single-channel recording of 14 μM DDHR in asolectin membranes. The current was recorded at 70 mV in 1 M KCl and 10 mM. The average pore conductance was 25 pS.

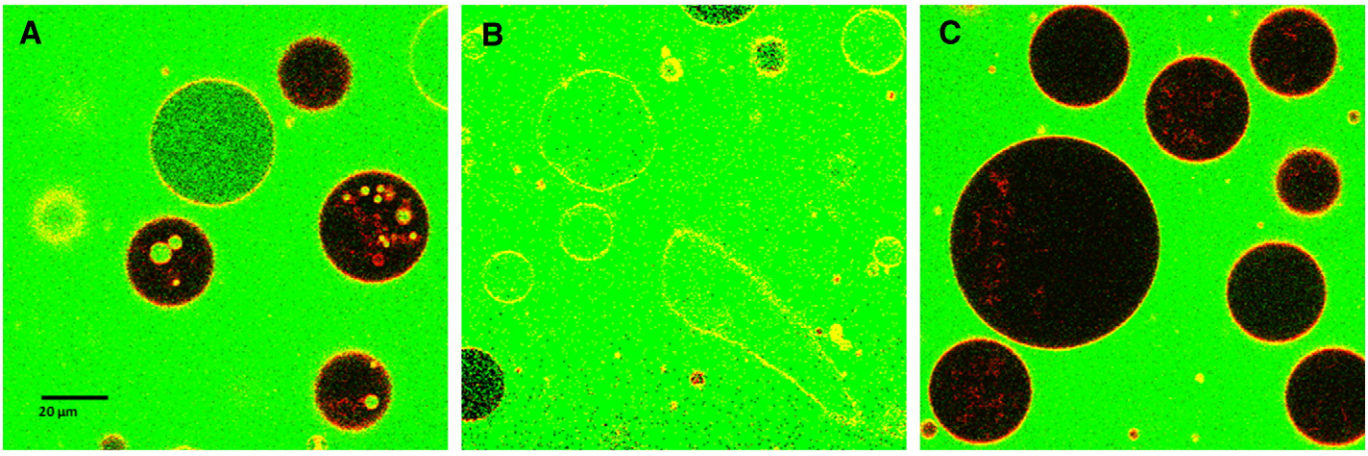

Fig. 6. Effect of DDHR on the shape of GUVs. The figure shows the most common morphological changes of GUVs that occurred at 30 μM DDHR. (A) Groups of small disorganized spheres observable inside the DOPC GUVs. (B) Irregularly elongated and asymmetric GUVs. (C) Stable DOPC/cholesterol GUVs without any significant changes in their shape or the formation of small spheres inside the vesicles. The green color represents the fluorescent probe (Atto488) used for the leakage assays.

inner leaflet. If the translocation is not favorable, spontaneous membrane curvature is established, compensating for the different area requirements of the two leaflets. Shape changes similar to those induced by DDHR have also been reported for azithromycin [25]. The authors showed a significant decrease in the elastic moduli of a DOPC bilayer upon the addition of azithromycin, and this decrease was accompanied by an increased area per DOPC headgroup. Computer modeling provides an explanation: azithromycin is horizontally located at the phospholipid acyl chain/headgroup interface. This results in an expansion of the outer leaflet and a decrease in DOPC–DOPC interactions, followed by the formation of buds. Thus, the observation of increased leaking after budding–fission cycles suggests another effective mechanism for membrane penetration in parallel to the mechanism of pore formation.

The cholesterol-containing GUVs remained stable at all concentrations of DDHR without any significant changes in their shape and the formation of small spheres inside the GUVs (Fig. 6C). Apparently, cholesterol prevents DDHR from imposing membrane curvature because cholesterol most likely provides DDHR with a translocation mechanism. The decreased leaking of cholesterol-containing GUVs upon DDHR treatment can also be attributed to the fact that the cholesterol-mediated stabilization of the bilayer does not allow other methods of membrane penetration except for pore formation, i.e., no leaking during the fission steps. The pores mediated by DDHR are less effective than the pores formed by AmB, which may be related to the ability of the mycosamine moiety to facilitate interactions between AmB and cholesterol [22].

In the cholesterol-containing GUVs, the presence of DDHR does not lead to the morphological changes observed in the DOPC bilayer; however, its action in the simple binary system of DOPC/Chol (7/3) is demonstrated by the phase separation of the bilayer. Fig. 7 shows a complementary pattern of DiD (L_d marker) and DDHR. To understand whether the phenomenon is caused by the generally higher ordering of the membrane or whether it arises from the favorable interaction between DDHR and cholesterol that seems to participate in the formation of pores, we also investigated the DDHR action in a pure POPC bilayer. The POPC bilayer displays a higher level of ordering that is not due to the presence of cholesterol but is due to the higher level of chain saturation. Surprisingly, as shown in Fig. 7, the phase separation also occurred in the POPC bilayer, providing clear evidence that the domains are not formed by a specific interaction with cholesterol but are formed due to the general physical properties of the membrane. Eventually, the morphological formations observed in DOPC GUVs were also observed in the POPC membrane. The extent of the formations was smaller; we mainly observed the loss of the round shape, and buds were not formed.

For the action of filipin III, a filipin-induced phase separation of cholesterol-containing membranes has been proposed [6] and has been observed using atomic force microscopy [5]. The phase separation of cholesterol-containing DOPC membranes can also be observed using fluorescence measurements in the presence of a much lower concentration (0.3 μM) of filipin III than in the case of the leakage experiments. However, Fig. 7 shows that the formation of DDHR-containing phases (or clusters) is not followed by the complementary changes in the DiD pattern, suggesting that the origin of the DDHR-induced changes differs from that for the filipin III observations, which were reported [26,27] to be driven by an interaction with cholesterol. No separation occurred when the system was treated with AmB.

3.5. Localization of DDHR in membranes

In the previous section, we discussed the involvement of DDHR in pore formation and the specific role of cholesterol. Here, we would like to examine the issue of DDHR partitioning into more rigid L_o lipid areas that are rich in cholesterol. GUVs composed of mixtures of unsaturated phosphatidylcholine, Sph and cholesterol are known for limited lipid miscibility and for phase separation [28].

To identify the preferential localization of DDHR, fluorescence images of DDHR were compared with images of the lipid tracer DiD, which has been shown to prefer the L_d phase [29]. Fig. 7 indicates that the localization of the two fluorescence molecules is complementary. The increased preference for the L_o phase itself is notable. It has been shown that most tail-labeled lipids, as well as organic dye molecules, preferentially segregate to the L_d phase [30]. This separation is attributed to the fact that more organized areas do not accommodate molecules, which would require the loss of the membrane order. The increased L_o partitioning is always attributed to a favorable spatial "matching" or even a specific interaction between the molecules of interest and the constituents of the L_o phase. Therefore, the L_o preference of DDHR, which is a relatively bulky molecule, would imply an interaction between DDHR and cholesterol. In contrast, in the case of AmB and filipin III, it has been proposed that sterols are merely responsible for a modulation of the bilayer properties that allow the bilayer to better accommodate the antibiotics [6,12]. It has to be admitted, however, that the direct interaction with cholesterol remains controversial.

We examined the DDHR distribution between two coexisting liquid phases in GUVs (the L_o and L_d phases) in vesicles made of ternary lipid

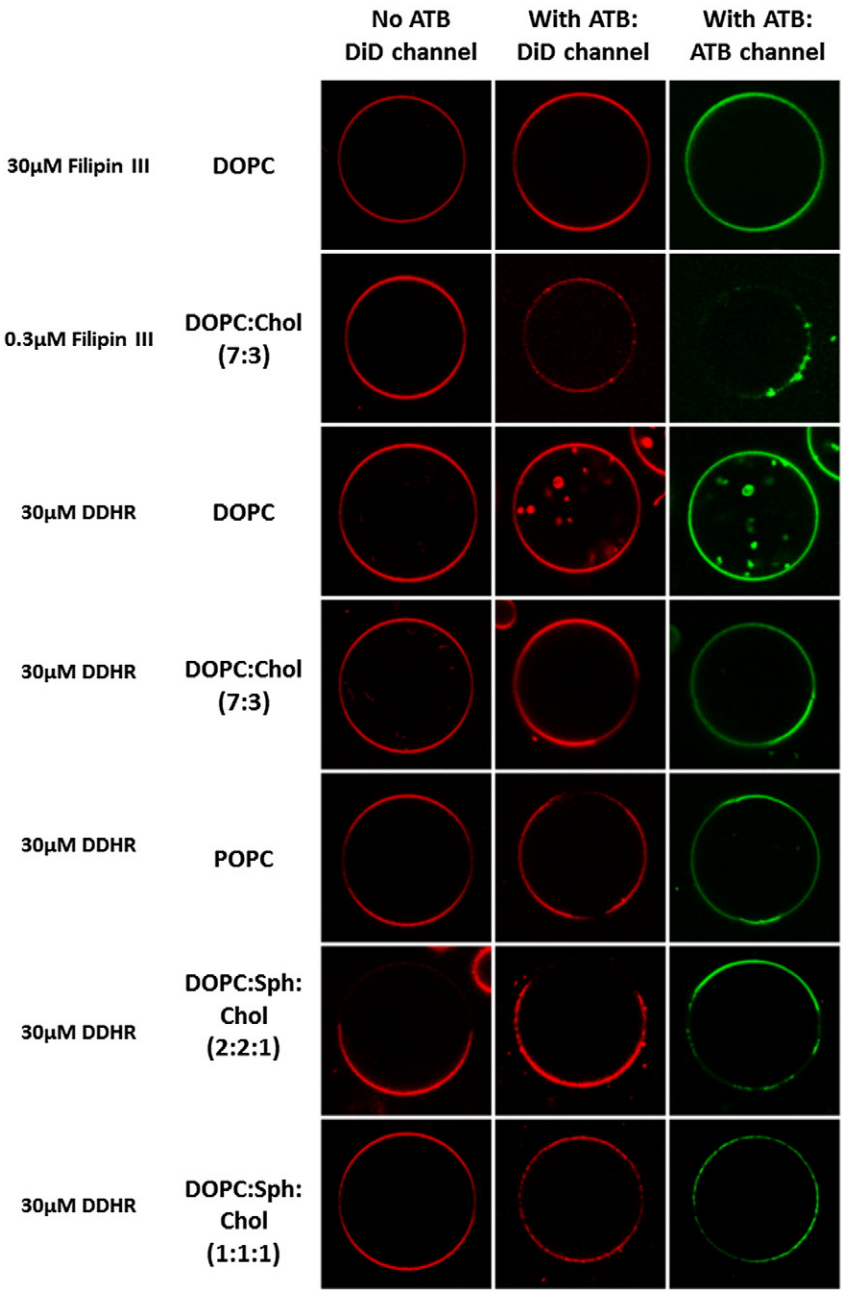

Fig. 7. Equatorial images of GUVs composed of various lipid mixtures. Images before and after the addition of selected antibiotics (ATB). The fluorescence recorded is in red for the DiD channel (L_d marker) and green for the ATB channel. Images of the green and red channels could not be taken simultaneously (the green and red channels are approximately 10 s delayed) due to the microscope setup used; thus, the images may correspond to slightly different z-optical sections and/or be moved in the xy-direction. Incubation time: 10 min.

mixtures (DOPC:Sph:cholesterol) in three different ratios—1:1:1, 1.5:1.5:1 and 2:2:1.

At larger amounts of Sph (the ratios 1.5:1.5:1 and 2:2:1), the GUVs exhibited a clear phase separation represented by the signal of DiD. DDHR localized in the areas without DiD fluorescence and did not appear to affect the size or geometry of the phases.

In GUVs with a lipid composition of 1:1:1 DOPC:Sph:cholesterol, no phase separation was observed before DDHR was added to the system. DiD was equally distributed over the entire surface of the vesicles. The addition of DDHR to the samples promoted the phase separation, and relatively small domains developed (Fig. 7). Thus, DDHR seems to substitute for the lack of Sph and facilitate the formation of the domains. The fact that the domains are small in size and also do not fuse suggests that DDHR stabilizes the domains at the L_d/L_o interface.

It is worth comparing the distribution coefficients of DDHR between the phases with and without Sph (DOPC/cholesterol). The values, which were calculated as the ratio of the mean DDHR fluorescence intensities in the two coexisting phases, are given in Fig. 8. The figure shows that for the larger Sph/cholesterol ratio, the contrast in the DDHR fluorescence between the cholesterol-rich and cholesterol-poor lipid phases is higher than that for the system consisting of only DOPC and cholesterol. This finding indicates that the DDHR localization is driven not only by the presence of sterols but also by the overall membrane properties.

The formation of membrane pores investigated by the leakage assay for the 1:1:1 composition is summarized in Table 1. Obviously, the presence of the L_o phases that recruit the majority of DDHR lowers the amount of leaking GUVs compared with that in the GUVs that are exclusively formed by DOPC.

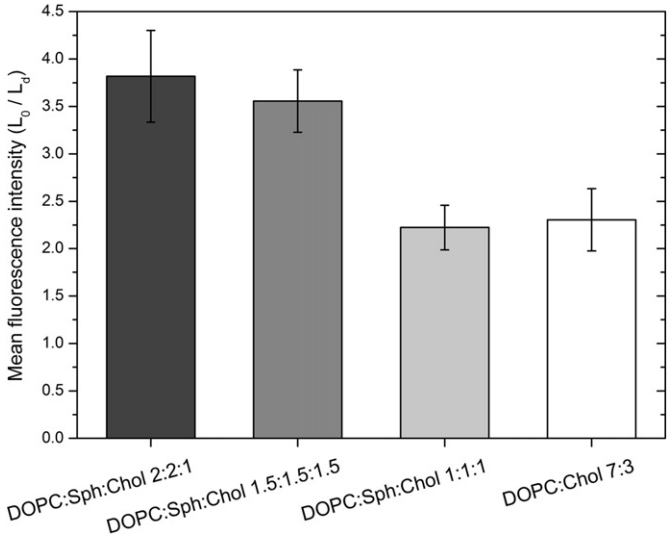

Fig. 8. The graph displays the ratio of mean of the DDHR fluorescence intensities in the coexisting Lo and Ld phases in GUVs with various compositions.

3.6. Interaction between DDHR and cholesterol

The measured FTIR spectra of DDHR in SDS clearly reflect the DDHR structure (Fig. 9) and show infrared bands similar to those of some related molecules, e.g., filipin III [31] or amphotericin B [32]. The DDHR infrared spectrum is dominated by strong bands for CH_2 stretching and CH_2 – OH vibrations at approximately 2924 cm^{-1}, carbonyl stretching vibrations at 1707 cm^{-1}, a region of CH_2 and CH_3 bending vibrations at approximately 1437 cm^{-1}, ester vibrations at ~1104 cm^{-1} and stretching vibrations of C – O – C in the pyranose ring at 1030 cm^{-1} (for the detailed band assignment, see Table **S1** in the Supplementary information).

The infrared spectrum after the addition of cholesterol to the buffer containing DDHR and SDS remains dominated by the DDHR spectrum (cf. Fig. 9A and B curves) because the infrared bands of cholesterol are less intense and prominent (Fig. **S1**). The FTIR difference spectrum, after the subtraction of the spectra of the independent components measured at the same conditions, clearly shows interactions between DDHR and cholesterol (Fig. 9C). (An independent subtraction without the baseline modification has been performed using the second derivative, which can identify overlapping components, with similar results—Fig. **S2** in the Supplementary information.)

The difference is dominated by changes in the DDHR bands. The most intense changes at 1642 cm^{-1} and 1575 cm^{-1} are associated with stretching C═O and C═C vibrations, respectively. An up-shift at 1276–1293 cm^{-1}, which most likely shows bending OH vibrations, an intensity change in the stretching C – O – C vibrations for the ester group at approximately 1164 cm^{-1} and bending CH vibrations at ca. 996 cm^{-1} are observed. The stretching CH_2 vibrations at 2849 cm^{-1} were downshifted, and the stretching CH_2 – OH vibrations at 2927 cm^{-1} were also affected by the binding. However, the interaction led to distinguishable band shifts for the cholesterol molecule. The most prominent cholesterol band at 1468 cm^{-1}, corresponding to bending CH_2 vibrations, and the band of stretching C – C vibrations of the aliphatic chain at 1066 cm^{-1} were shifted to higher wavenumbers.

Considering all these FTIR spectral changes that occur when DDHR interacts with cholesterol in the SDS buffer, we may conclude that cholesterol most likely primarily binds to the ester part of the DDHR molecule, helping the DDHR molecule to organize itself into a more planar and rigid molecule. Nevertheless, subsequent interactions of the more rigid DDHR with other free DDHR molecules cannot be excluded.

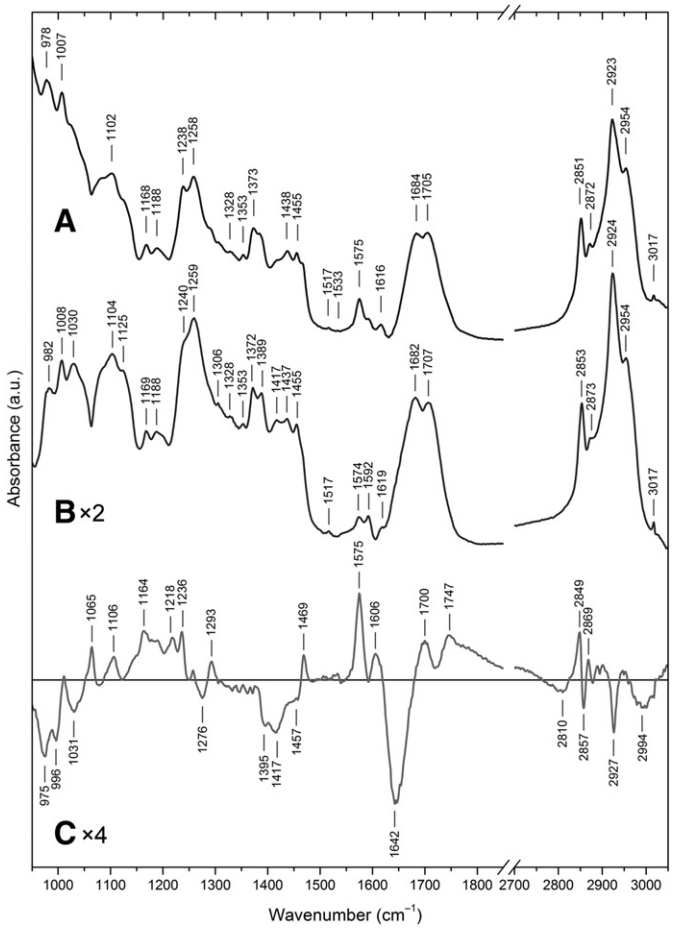

Fig. 9. The FTIR spectra of (A) 40 mM DDHR with 40 mM cholesterol in 80 mM SDS buffer and (B) 40 mM DDHR in 80 mM SDS buffer. (C) The difference of (A) minus (B) and minus the FTIR spectrum of 40 mM cholesterol in 80 mM SDS buffer (Fig. S1 in Supplementary information) and the polynomial fit of a 7th grade. (The zero level is marked for the difference.)

The FTIR experiments require concentrations of the investigated compounds that are more than three orders of magnitude higher than those for the microscopy experiment. Performing these experiments in lipid vesicles with similar lipid-to-cholesterol ratios would not be feasible; therefore, SDS is required to solubilize the compounds. Therefore, the FTIR data cannot prove that DDHR interacts with cholesterol in the biological membrane. These data can, however, indicate what vibrations would most likely participate in that interaction. Our leakage experiments strongly suggest that cholesterol plays a distinct role in the formation of DDHR pores, and this formation may be mediated by the interaction observed in the FTIR measurements.

4. Conclusions

In this work, we have investigated the membrane action of a newly isolated member of the polyene macrolide family, DDHR. In particular, we have focused on its involvement in pore formation, the morphological changes it imposes on model GUV membranes, its partitioning between various fluid lipid phases and its ability to initiate the formation of these phases. In addition, we have studied the role of cholesterol in all the specified issues.

Our leakage assays show that DDHR triggers pore formation independently of the presence of cholesterol. However, the pores only seem to have a distinct size and temporal stability in the cholesterol-containing bilayers. Without cholesterol, the pore size depends on the DDHR concentration, and the pores are transient, as suggested by the

conductance measurements of BLMs. Moreover, the leakage in the absence of cholesterol is also dependent on other leaking mechanisms, as indicated by the budding/fission-associated permeation. Although the formation of buds becomes suppressed in membranes that have higher rigidity irrespective of the presence of cholesterol, the formation of pores has a distinct, cholesterol-specific character.

DDHR preferentially inserts into membrane areas that have higher lipid order, and in addition, the insertion leads to phase separation in membranes with a lipid composition close to the phase separation boundary (DOPC/Sph/Chol 1/1/1). Surprisingly, however, the phase separation also occurs in DOPC/Chol (7/3) and pure POPC membranes. This result demonstrates a highly organizing effect of DDHR that requires a certain degree of membrane rigidity, but this effect is not associated solely with the presence of cholesterol.

Acknowledgments

Financial support was provided by the Czech Science Foundation (14-03141J to Š.P. and J.H., P207/12/P890 to R.F.), the Grant Agency of the Charles University (1334614 to A.K.), a Charles University grant SVV 260083 (to A.K. and J.Č.), Charles University Projects (UNCE 204013/2012 to J.Č. and A.K.), the European Regional Development Fund (BIOCEV CZ.1.05/1.1.00/02.0109 to J.Č. and A.K.), and the Ministry of Education, Youth and Sports of the Czech Republic (LH 13259 KONTAKT to M.H.). Moreover, the Academy of Sciences for the Praemium Academie award is acknowledged (M.H.).

Appendix A. Supplementary data

Supplementary data to this article can be found online at http://dx.doi.org/10.1016/j.bbamem.2014.10.038.

References

[1] J.F. Aparicio, P. Caffrey, J.A. Gil, S.B. Zotchev, Polyene antibiotic biosynthesis gene clusters, Appl. Microbiol. Biotechnol. 61 (2003) 179–188.
[2] J. Bolard, How do the polyene macrolide antibiotics affect the cellular membrane-properties, Behav. Ecol. Sociobiol. 864 (1986) 257–304.
[3] A. Coutinho, M. Prieto, Cooperative partition model of nystatin interaction with phospholipid vesicles, Biophys. J. 84 (2003) 3061–3078.
[4] J. Milhaud, Permeabilizing action of filipin-III on model membranes through a filipin-phospholipid binding, Behav. Ecol. Sociobiol. 1105 (1992) 307–318.
[5] N.C. Santos, E. Ter-Ovanesyan, J.A. Zasadzinski, M. Prieto, M.A.R.B. Castanho, Filipin-induced lesions in planar phospholipid bilayers imaged by atomic force microscopy, Biophys. J. 75 (1998) 1869–1873.
[6] S.C.D.N. Lopes, E. Goormaghtigh, B.J.C. Cabral, M.A.R.B. Castanho, Filipin orientation revealed by linear dichroism. Implication for a model of action, J. Am. Chem. Soc. 126 (2004) 5396–5402.
[7] D. Gottlieb, H.E. Carter, J.H. Sloneker, A. Ammann, Protection of fungi against polyene antibiotics by sterols, Science 128 (1958) 361-361.
[8] J.O. Lampen, E.R. Morgan, A. Slocum, P. Arnow, Absorption of nystatin by microorganisms, J. Bacteriol. 78 (1959) 282–289.
[9] G. Weissman, G. Sessa, Action of polyene antibiotics on phospholipid-cholesterol structures, J. Biol. Chem. 242 (1967) 616.
[10] Hamilton-Miller J.M., Chemistry and biology of polyene macrolide antibiotics, Bacteriol. Rev. 37 (1973) 166–196.
[11] J.O. Lampen, P.M. Arnow, R.S. Safferman, Mechanism of protection by sterols against polyene antibiotics, J. Bacteriol. 80 (1960) 200–206.
[12] B. Venegas, J. Gonzalez-Damian, H. Celis, I. Ortega-Blake, Amphotericin B channels in the bacterial membrane: role of sterol and temperature, Biophys. J. 85 (2003) 2323–2332.
[13] N. Matsumori, Y. Sawada, M. Murata, Mycosamine orientation of amphotericin B controlling interaction with ergosterol: sterol-dependent activity of conformation-restricted derivatives with an amino-carbonyl bridge, J. Am. Chem. Soc. 127 (2005) 10667–10675.
[14] E. Stodulkova, M. Kuzma, I.B. Hench, J. Cerny, J. Kralova, P. Novak, M. Chudickova, M. Savic, L. Djokic, B. Vasiljevic, M. Flieger, New polyene macrolide family produced by submerged culture of *Streptomyces durmitorensis*, J. Antibiot. 64 (2011) 717–722.
[15] N. Stankovic, L. Senerovic, Z. Bojic-Trbojevic, I. Vuckovic, L. Vicovac, B. Vasiljevic, J. Nikodinovic-Runic, Didehydroroflamycoin pentaene macrolide family from *Streptomyces durmitorensis* MS405(T): production optimization and antimicrobial activity, J. Appl. Microbiol. 115 (2013) 1297–1306.
[16] M.I. Angelova, S. Soleau, P. Meleard, J.F. Faucon, P. Bothorel, Preparation of giant vesicles by external Ac electric-fields—kinetics and applications, Trends Colloid Interf. Sci. VI 89 (1992) 127–131.
[17] V. Weissig, Liposomes: methods and protocols, Biological Membrane Models, vol. 2, Humana Press, New York, 2010.
[18] M.J. Hope, M.B. Bally, L.D. Mayer, A.S. Janoff, P.R. Cullis, Generation of multilamellar and unilamellar phospholipid-vesicles, Chem. Phys. Lipids 40 (1986) 89–107.
[19] F. Dousseau, M. Therrien, M. Pezolet, On the spectral subtraction of water from the Ft-Ir spectra of aqueous-solutions of proteins, Appl. Spectrosc. 43 (1989) 538–542.
[20] M.A.R.B. Castanho, A. Coutinho, M.J.E. Prieto, Absorption and fluorescence-spectra of polyene antibiotics in the presence of cholesterol, J. Biol. Chem. 267 (1992) 204–209.
[21] A. Coutinho, L. Silva, A. Fedorov, M. Prieto, Cholesterol and ergosterol influence nystatin surface aggregation: relation to pore formation, Biophys. J. 87 (2004) 3264–3276.
[22] D.S. Palacios, I. Dailey, D.M. Siebert, B.C. Wilcock, M.D. Burke, Synthesis-enabled functional group deletions reveal key underpinnings of amphotericin B ion channel and antifungal activities, Proc. Natl. Acad. Sci. U. S. A. 108 (2011) 6733–6738.
[23] C.D. Stubbs, T. Kouyama, K. Kinosita, A. Ikegami, Effect of double-bonds on the dynamic properties of the hydrocarbon region of lecithin bilayers, Biochemistry 20 (1981) 4257–4262.
[24] M. Nazari, M. Kurdi, H. Heerklotz, Classifying surfactants with respect to their effect on lipid membrane order, Biophys. J. 102 (2012) 498–506.
[25] N. Fa, L. Lins, P.J. Courtoy, Y. Dufrene, P. Van Der Smissen, R. Brasseur, D. Tyteca, M.P. Mingeot-Leclercq, Decrease of elastic moduli of DOPC bilayers induced by a macrolide antibiotic, azithromycin, Biochim. Biophys. Acta Biomembr. 1768 (2007) 1830–1838.
[26] A.W. Norman, Vandeene Ll, B. Dekruyff, R.A. Demel, Journal of Biological Chemistry, Studies on biological properties of polyene antibiotics—evidence for direct interaction of filipin with cholesterol, J. Biol. Chem. 247 (1972) 1918.
[27] M. Castanho, M. Prieto, Filipin fluorescence quenching by spin-labeled probes—studies in aqueous-solution and in a membrane model system, Biophys. J. 69 (1995) 155–168.
[28] S.L. Veatch, S.L. Keller, Miscibility phase diagrams of giant vesicles containing sphingomyelin, Phys. Rev. Lett. 94 (2005) 148101.
[29] S. Chiantia, J. Ries, N. Kahya, P. Schwille, Combined AFM and two-focus SFCS study of raft-exhibiting model membranes, ChemPhysChem 7 (2006) 2409–2418.
[30] E. Sezgin, I. Levental, M. Grzybek, G. Schwarzmann, V. Mueller, A. Honigmann, V.N. Belov, C. Eggeling, U. Coskun, K. Simons, P. Schwille, Partitioning, diffusion, and ligand binding of raft lipid analogs in model and cellular plasma membranes, Biochim. Biophys. Acta Biomembr. 1818 (2012) 1777–1784.
[31] G.B. Whitfield, T.D. Brock, A. Ammann, D. Gottlieb, H.E. Carter, Filipin, an antifungal antibiotic—isolation and properties, J. Am. Chem. Soc. 77 (1955) 4799–4801.
[32] M. Gagos, M. Arczewska, FTIR spectroscopic study of molecular organization of the antibiotic amphotericin B in aqueous solution and in DPPC lipid monolayers containing the sterols cholesterol and ergosterol, Eur. Biophys. J. Biophys. Lett. 41 (2012) 663–673.